IOP Publishing Plasma Sources Science and Technology
Plasma Sources Sci. Technol. **27** (2018) 095014 (8pp) https://doi.org/10.1088/1361-6595/aadf56

Evaluating microgap breakdown mode transition with electric field non-uniformity

Yangyang Fu[1,2], Janez Krek[1], Peng Zhang[2] and John P Verboncoeur[1,2]

[1] Department of Computational Mathematics, Science and Engineering, Michigan State University, East Lansing, MI 48824, United States of America
[2] Department of Electrical and Computer Engineering, Michigan State University, East Lansing, MI 48824, United States of America

E-mail: fuyangya@egr.msu.edu

Received 29 July 2018, revised 22 August 2018
Accepted for publication 6 September 2018
Published 25 September 2018

Abstract

This paper evaluates the transitions between the breakdown modes that are dominated by field emission (FE) and by secondary electron emission (SEE) in argon microgaps, based on a mathematical model originally proposed for the modified Paschen's curve (Go and Pohlman 2010 *J. Appl. Phys.* **107** 103303). In the present model, instead of assuming a constant electric field across the gap, the spatial distribution of the electric field due to the presence of a parabolic cathode protrusion is implemented, and a modification of the first Townsend ionization coefficient for microscale gaps from particle-in-cell/Monte Carlo collision simulations is employed (Venkattraman and Alexeenko 2012 *Phys. Plasmas* **19** 123515). The breakdown mode transitions are quantified by the variations of gas pressure and gap distance. It is found that assuming a constant electric field across the gap will overestimate the electron avalanche, which underestimates the breakdown voltage and shifts the breakdown mode transitions to a smaller gap. By varying the field enhancement factor, the critical point of the breakdown mode transition can be significantly adjusted. Increasing the field enhancement factor will lower the breakdown voltage in the FE regime and increase the breakdown voltage in the SEE regime.

Keywords: gas breakdown, Paschen's law, microdischarge, field emission, Townsend discharge, secondary electron emission, breakdown mode transition

1. Introduction

The gas breakdown mechanisms in microgaps (less than 10 μm) transiting from the field emission (FE) dominant regime to the secondary electron emission (SEE) dominant regime are widely reported both experimentally and numerically [1–5]. Understanding these phenomena is of critical importance for many prospective applications in nano- and micro-scale electronics, including micro-electro-mechanical systems, micro-switches, and microchip devices [6–10]. As previously reported, the Townsend theory for microdischarges holds until field emission becomes dominant [11–13]. The key physical mechanisms for the breakdown processes are the electron avalanche process (the α process) across the gap and the surface emission processes (the γ process, such as SEE and FE) at the cathode. The α process combined with the SEE and the FE results in microgap breakdown in different regimes.

Deviations from Paschen's law of gas breakdown in the presence of field emission were observed in the 1950s [14–17]. To elucidate the breakdown deviations with field emission, an empirical form for the electron current density driven by the cathode electric field was proposed by Boyle and Kisliuk [15]. Based on this empirical form, Ramilović-Radjenović and Radjenović derived a mathematical model for microgap breakdown caused by ion-enhanced field emission, which agrees with the particle-in-cell/Monte Carlo collision (PIC/MCC) model when the discharge is in the field emission regime [18–20]. However, as Ramilović-Radjenović and Radjenović mentioned in [19], this model will overestimate the breakdown voltage as the gap distance increases where the field emission gradually disappears and the SEE becomes

dominant. Later in [21, 22], Go, Pohlman, and Tirumala proposed a formulation of the so-called modified Paschen's curve, combining the field emission and the SEE coefficients into the Townsend breakdown criteria, which successfully describes the breakdown mode transition between the field emission regime and the SEE regime. In that model, the Fowler–Nordheim (F–N) equation is employed to describe the field emission current density and the impact of the uncertainty of the related parameters, such as work function, field enhancement factor, and other fitting parameters, on the breakdown curves has been assessed [22–24]. One limitation of the model is that the electric field is treated as a constant across the gap and it is suddenly enhanced at the cathode by an assumed factor. Though making the formula simple and generally clear, the assumption of constant electric field is physically less appropriate and often violated, which might result in unexpected misbehaviors in calculating the breakdown voltages. The effect of the electric field non-uniformity on Paschen's curve in macrogaps can be found in [25–29].

In this work, the non-uniformity of the electric field across the gap due to the presence of a parabolic cathode tip is considered for calculations of the cathode field emission and the first Townsend ionization coefficient. The contributions from the field emission and the SEE on the electron avalanche are evaluated in argon microgap breakdowns. The breakdown mode transitions are quantified by the variations of the gas pressure and the gap distance. In section 2, the mathematical model for microgap breakdown is introduced and the treatment of the electric field and the first Townsend ionization coefficient is discussed. In section 3, Paschen's curves calculated using different ionization coefficients are compared, followed by the evaluation of the transition characteristics of the discharge from the FE regime to the SEE regime. The effects of the non-uniform electric field and the field enhancement factor are also discussed. Concluding remarks are given in section 4.

2. Mathematical model

In Townsend gas breakdowns, the α process leads to electron impact ionization across the gap and the γ process results in electron emissions from the cathode, both of which are important for self-sustained discharges [30–32]. Depending on the discharge conditions, the cathode emission could be either ion-enhanced field emission or ion-induced SEE. The first Townsend ionization coefficient α is used to describe the electron-impact ionization during avalanches, which is given by

$$\alpha = Ap\exp(-Bpd/U), \tag{1A}$$

or

$$\alpha = Cp\exp(-D\sqrt{pd/U}), \tag{1B}$$

where A, B, C, and D are constants based on the gas type, p is the gas pressure, d is the gap distance, and U is the applied voltage in the gap [21]. Note that equation (1*A*) is widely used and assumes that the electrons undergo only ionizing collisions, which may be realistic at high reduced electric fields and moderate energies; equation (1*B*) is usually used for inert gas since it gives a better fit to the experimental data [32]. For the gap with uniform electric field, the Townsend avalanche criteria for gas breakdown is expressed as

$$\gamma_{\mathrm{SEE}}(\mathrm{e}^{\alpha d} - 1) = 1, \tag{2}$$

where γ_{SEE} is the SEE coefficient that depends on both cathode material and the gas. Combining equations (1*A*) and (2) yields the conventional Paschen's curve

$$U_b = \frac{Bpd}{\ln(pd) + \ln\left[\frac{A}{\ln(1/\gamma_{\mathrm{SEE}}+1)}\right]}. \tag{3}$$

Equation (3) describes the breakdown voltage when cathode emission only includes SEE [31, 32]. When the microgap size becomes smaller than several microns (or equivalently, the electric field strength is on the order of 10^9 V m^{-1}), field emission can also contribute to the cathode emission. The FE current density j_{FN} described by the F–N equation is

$$j_{\mathrm{FN}} = \frac{A_{\mathrm{FN}}\beta^2E^2}{\varphi t^2(y)}\exp\left[-\frac{B_{\mathrm{FN}}\varphi^{3/2}\upsilon(y)}{\beta E}\right], \tag{4}$$

where A_{FN} and B_{FN} are the F–N constants, E is the applied electric field defined as $E = U/d$, φ is the work function of the cathode, and β is the local field enhancement factor. The parameter y is a function of φ, β, and E, and the barrier shape function $t^2(y)$ and $\upsilon(y)$ have established approximations [33, 34]. Using this field emission expression, the effective field emission coefficient is given by

$$\gamma_{\mathrm{FE}} = K\exp\left(-\frac{D_{\mathrm{FN}}}{E}\right), \tag{5}$$

where K and D_{FN} are material and gas dependent constants. The constant K is related to the ion enhancement effect and can be determined from the ratio of the field emission current density to the positive ion current density into the cathode [19]. However, the experimental determination may be quite difficult since there are complications due to electron attachment, ionization by metastables, etc [18–20]. In this study, K is treated as a constant much larger than 1 ($\sim 10^7$) and D_{FN} is defined as [15, 21]

$$D_{\mathrm{FN}} = (6.85\times 10^9)\frac{\varphi^{3/2}}{\beta}. \tag{6}$$

The modified breakdown criteria, which includes FE-driven and SEE-driven breakdown, is given by Go and Pohlman as follows [21]

$$(\gamma_{\mathrm{SEE}} + \gamma_{\mathrm{FE}})(\mathrm{e}^{\alpha d} - 1) = 1. \tag{7}$$

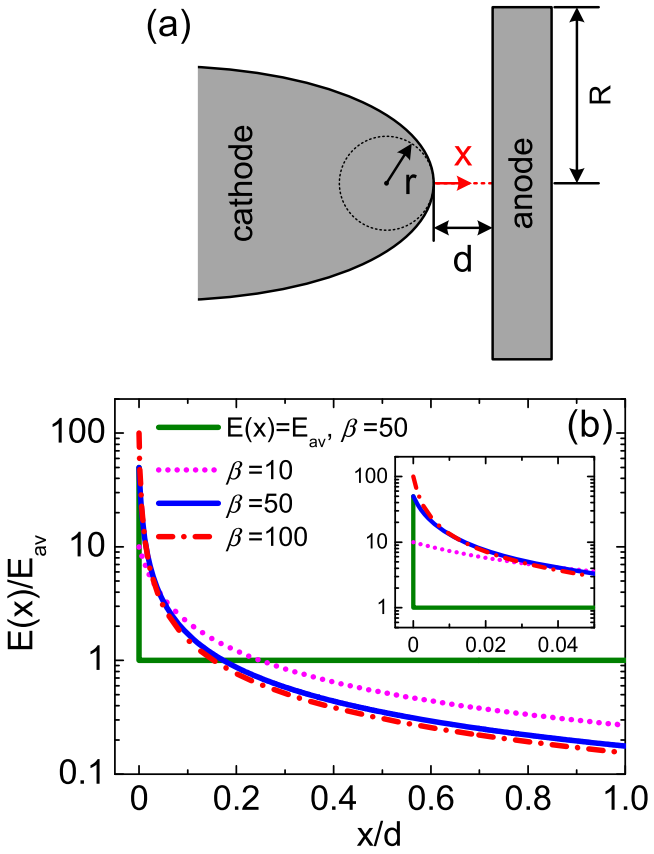

Figure 1. (a) Schematic of the anode-cathode microgap where x is the distance from the protrusion tip along the axis, d is the gap distance, r is the curvature radius, and R is the anode radius ($R \gg d$); (b) normalized uniform electric field distribution with $\beta = 50$ and normalized non-uniform electric field distributions using equation (8) with $\beta = 10$, 50, and 100, respectively. $x/d = 0$ is the cathode tip and $x/d = 1.0$ is the anode.

Substituting equation (1*A*) into (7) yields the modified Paschen's curve transiting from the FE dominant regime to the SEE dominant regime. This model was verified to be qualitatively correct and the complete details of the model can be found in [21, 22]. However, the model can be more reasonable and universal if the electric field non-uniformity is included, rather than assuming uniform electric field across the gap. This uniform electric filed assumption results in the first Townsend coefficient being a constant across the gap and cannot reflect the spatial dependence of the Townsend coefficient when the electric field is not uniform, which is the case with the presence of surface protrusions or surface roughness. Thus, a spatially-dependent electric field $E = E(x)$, rather than $E = U/d$, should be employed to capture the breakdown characteristic with the electric field non-uniformity. The nonlocal field effects have a big impact on the Townsend coefficient α, which could change the breakdown characteristics significantly when the contribution from the electron avalanche becomes dominant. In other words, the nonlocal field effects will become important when the electron mean free path λ is comparable to or smaller than the length scale over which the electric field changes.

In order to consider the effect of the non-uniformity of the electric field, a parabolic surface protrusion as the cathode facing an infinite plane electrode is employed, as shown in figure 1(a), where x is the distance from the protrusion tip along the axis, d is the gap distance, r is the curvature radius, and R is the anode radius ($R \gg d$). The electric field distribution along the axis is given by [32]

$$E(x) = \frac{2U}{(2x + r)\ln(2d/r + 1)}. \tag{8}$$

For a given gap distance d, an expected field enhancement factor β at the cathode can be achieved by adjusting the geometry parameter r in equation (8), i.e., $\beta = (2d/r)/\ln(2d/r + 1)$. Note that in this model, the field enhancement factor is only due to the geometrical effects and works as an effective global field enhancement factor. The field enhancements caused by surface morphology, electrical heterogeneity, and work function variation are not included and the contributions from the microscopic and macroscopic enhancement are not distinguished [35–37]. Figure 1(b) shows the normalized uniform electric field distribution with $\beta = 50$ and normalized non-uniform electric field distributions using equation (8) with $\beta = 10$, 50, and 100, respectively. It can be seen that for a given field enhancement, the electric field decays across many orders of magnitude from the cathode ($x/d = 0$) to the anode ($x/d = 1.0$), showing non-uniform behaviors of distributions. A larger field enhancement near the cathode will lead to a faster decay of the electric field towards the anode.

Besides the consideration of electric field non-uniformity, the semi-empirical formulas for the Townsend coefficient in macrogaps, given by equations (1*A*) and (1*B*), might be modified to more accurately describe discharges in microgaps. In the microscale regime, when the applied voltage is small (comparable to the ionization potential), the effect of backscattering becomes particularly important since the elastic scattering of low-energy electrons is largely isotropic, which results in a reasonable fraction of backscattered electrons drifting towards the cathode [38]. Therefore, without considering the backscattering effect, using a macroscale ionization expression for microgap will overestimate the first Townsend ionization coefficient. Using PIC/MCC simulations, a semi-empirical formula with a correction term is given for microgaps, accounting for the significantly smaller number of collisions

$$\left(\frac{\alpha}{p}\right)_{\text{micro}} = \left(\frac{\alpha}{p}\right)_{\text{macro}}\left[1 - \exp\left(-\left(\frac{U/\Psi_i - 1}{3.1}\right)^{0.8}\right)\right], \tag{9}$$

where Ψ_i refers to the gas ionization potential in units of V and $(\alpha/p)_{\text{macro}}$ can be given by either equation (1*A*) or (1*B*) [24, 38]. For argon, extending equation (1*B*) with non-uniform electric field, the value of macroscale $\alpha(x)$ is given by

$$\alpha(x)_{\text{macro}} = Cp\exp\left(-D\sqrt{p/E(x)}\right), \tag{10}$$

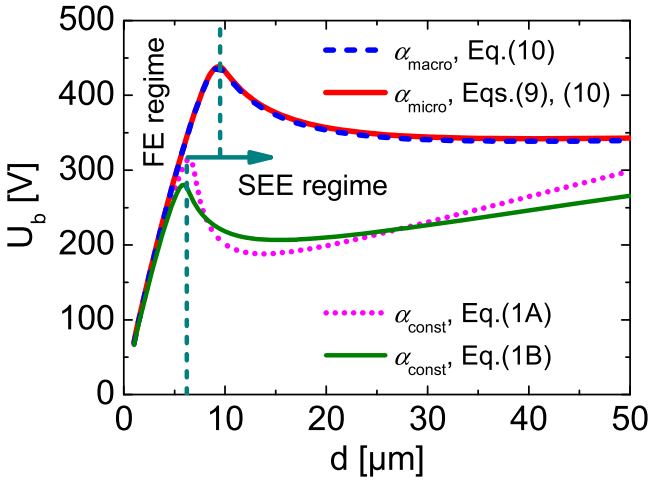

Figure 2. Calculated Paschen's curves using different Townsend ionization coefficients for argon. α_{const} from equations (1*A*) or (1*B*) does not take into account of the electric field non-uniformity, α_{macro} from equation (10) includes the effect of the electric field non-uniformity, and α_{micro} from equations (9) and (10) includes the modification of α from macroscale to microscale. In the calculation, $p = 760$ Torr, $\gamma_{\text{SEE}} = 0.01$, $\beta = 50$, $\varphi = 4.0$ eV, and $K = 10^7$.

where $C = 29.2$ Torr^{-1} cm^{-1} and $D = 26.6$ V$^{1/2}$ Torr$^{-1/2}$ cm$^{-1/2}$, which is considered to lead to better agreement with experiments for inert gases [32, 38]. The modification for the Townsend ionization coefficient is indispensable especially when the microgap becomes ultra small (less than ~3 μm) and the applied voltage is comparable to the ionization potential.

Combining the equations (7)–(10), the breakdown criteria is expressed as

$$\left[\gamma_{\text{SEE}} + K\exp\left(-\frac{6.85 \times 10^9 \varphi^{3/2}}{E_{\text{cathode}}}\right)\right] \times \left[\exp\left(\int_0^d \alpha_{\text{micro}}(x) \cdot \mathrm{d}x\right) - 1\right] = 1, \tag{11}$$

where $E_{\text{cathode}} = E(x)|_{x=0}$ is the cathode electric field and $\alpha_{\text{micro}}(x) = f(E(x)/p)$ is a function of the spatially-dependent reduced electric field, given by equations (9) and (10). The breakdown voltage can be obtained by solving the transcendental equation (11) numerically.

3. Results and discussion

First, the previous model with constant electric field was rebuilt and the Paschen's curve using α_{const} was reproduced for air (not presented here), confirming the results are identical to the results in [21]. In the following calculations, argon was the working gas and $\gamma_{\text{SEE}} = 0.01$, $\beta = 50$, $\varphi = 4.0$ eV, and $K = 10^7$ are used, unless stated otherwise. Three different Townsend coefficients are used when solving the equation (11). The spatially-independent α_{const} is calculated with constant electric field across the gap using equations (1*A*) or (1*B*), respectively; two spatially-dependent coefficients: $\alpha(x)_{\text{macro}}$ is calculated using equation (10) and $\alpha(x)_{\text{micro}}$ is calculated using equation (9) with $\alpha(x)_{\text{macro}}$ from equation (10).

Figure 2 shows the breakdown voltage curves calculated for argon at atmospheric pressure by using different Townsend ionization coefficients. It can be seen that the three breakdown curves generally have similar trends, transiting from the FE regime to the SEE regime, as the gap distance increases. In the FE regime, all the four breakdown voltages are very close until the one using α_{const} changes the breakdown mode (reaching the maximum breakdown voltage). With the constant electric field, the Paschen's curves using α_{const} from equations (1*A*) and (1*B*) are slightly different but the critical points of the breakdown mode transition are quite close. With the inclusion of the electric field non-uniformity, the breakdown mode transition occurs at a larger gap distance (~10 μm), and in the SEE regime, the breakdown voltages are larger than that with α_{const}. This is due to the fact that with the same voltage across the gap, assuming the uniform electric field overestimates the electron avalanche ionization, which in turn underestimates the breakdown voltage especially when the discharge enters the SEE regime. The breakdown curves with α_{micro} and α_{macro} are basically the same, which is explained below by the spatial distributions of the first Townsend ionization coefficients.

Figure 3 shows spatial distributions of $(\alpha/p)_{\text{macro}}$ and $(\alpha/p)_{\text{micro}}$ for gap distance d varying from 1 to 50 μm, with applied voltage $U = U_b$ and gas pressure $p = 760$ Torr. The two coefficients are different when the gap distance is ultra small (<~3 μm), whereas almost the same when the gap distance is larger. With $d < 3$ μm, α_{micro} is much lower than α_{macro} in most of the gap, which is closely related to the ratio of the ionization mean free path to the gap size ($d/\lambda \sim U/\Psi_{\text{i}}$) [38]. As mentioned before, the modification with equation (9) becomes noticeable when the breakdown voltage U_b is comparable to the gas ionization potential Ψ_{i}, i.e., the d/λ is not much larger than 1. As the gap distance increases, U_b becomes much larger than Ψ_{i} (for argon $\Psi_{\text{i}} = 15.6$ V), the modification factor in the equation (9) is close to 1. Thus, the difference between two coefficients gradually disappears as the gap distance increases. Note that the field emission from equation (5) is very sensitive to the electric field and a small variation in the applied voltage can significantly change the field emission coefficient. The difference in Townsend ionization coefficient in the FE regime is less important and has little impact on the breakdown voltage at this pressure. This also explains why the Paschen's curves from α_{macro} and α_{micro} in figure 2 are basically the same in both the FE regime and the SEE regime.

When solving equation (11), the electron avalanche and the field emission are evaluated and presented in figure 4 to show the individual contributions of the α process and the γ process, respectively. A parameter to describe the field emission contribution (FE Contri.) is defined as

$$\text{FE Contri.} = \frac{\gamma_{\text{FE}}}{\gamma_{\text{SEE}} + \gamma_{\text{FE}}}. \tag{12}$$

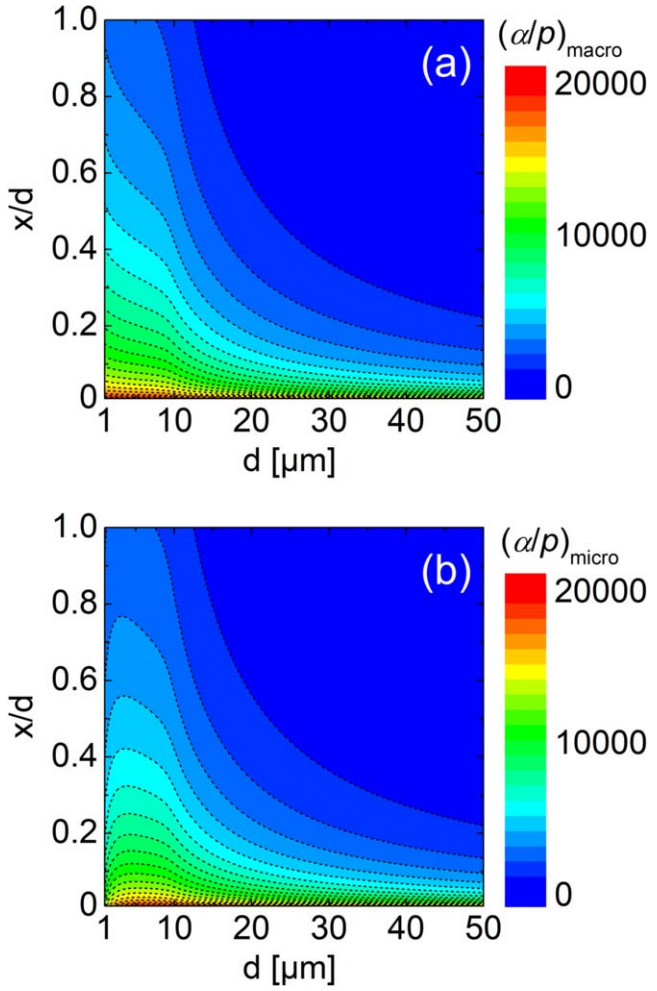

Figure 3. Comparison of the Townsend ionization coefficient α/p (in the unit of cm^{-1} $Torr^{-1}$) using (a) equation (10) for macroscale gaps and (b) equations (9) and (10) for microscale gaps. In the calculation, $\beta = 50$, $p = 760$ Torr, and the applied voltage is equal to the breakdown voltage.

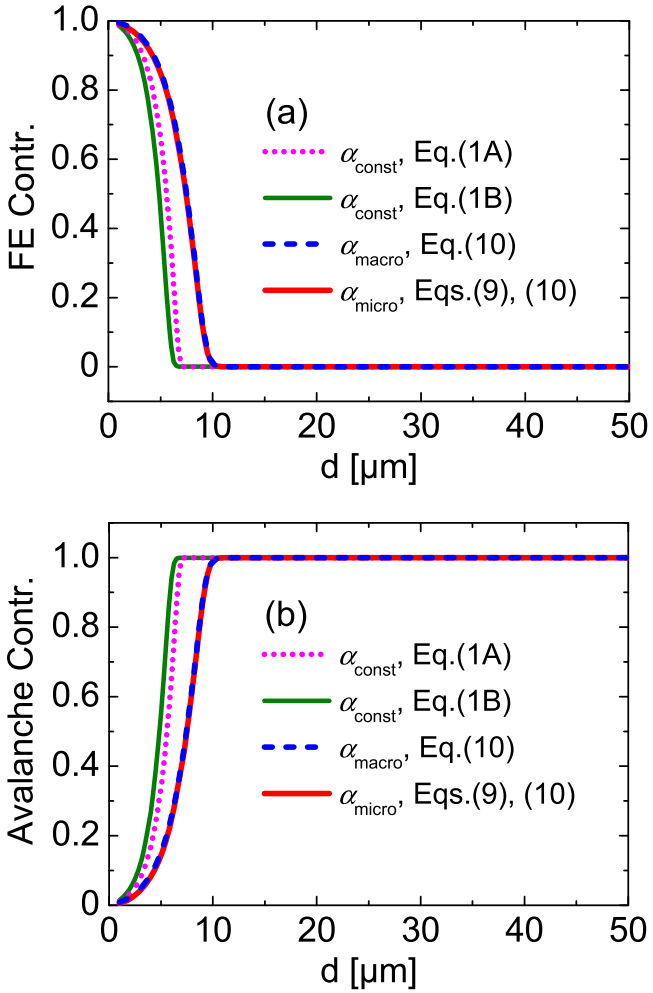

Figure 4. Evaluation of contributions of the field emission (a) and the electron avalanche (b) to the breakdown criteria. In the calculation, $p = 760$ Torr, $\gamma_{SEE} = 0.01$, $\beta = 50$, $\varphi = 4.0$ eV, and $K = 10^7$.

This parameter can explicitly show which regime is dominant and also the breakdown mode transition between the FE regime and the SEE regime. In figure 4(a), the comparisons are made with different Townsend coefficients. It can be seen that the field emission contribution disappears when the gap distance is larger than 10 μm, and by ignoring the non-uniformity of the electric field, it will predict the breakdown mode transition occurring with a smaller d, which is consistent with the results in figure 2.

The electron avalanche contribution (Avalanche Contri.) is defined as

$$\text{Avalanche Contri.} = \frac{\exp\left(\int_0^d \alpha(x)\cdot \mathrm{d}x\right) - 1}{M_{\text{limit}}}, \qquad (13)$$

where M_{limit} is the limit of the electron avalanche without the field emission. The SEE is always included (usually as a constant γ_{SEE}), even in the FE regime, thus the limit of the electron avalanche should be $M_{\text{limit}} = 1/\gamma_{SEE}$ for the breakdowns when the field emission is ignorable. In figure 4(b), as the gap distance increases, the electron avalanche contribution increases in the transitions from the FE regime and reaches its limit in the SEE regime. Comparing figures 4(a) and (b), the electron avalanche and the field emission counterbalance with each other to satisfy equation (11) and the breakdown mode transitions are found to be self-consistent.

The Paschen's curves calculated by changing the gas pressure for a fixed gap distance are shown in figure 5. The gap distance is fixed at 1, 2, and 3 μm with the pd varying in the range of 0.01–2.0 Torr cm. Other related parameters in equations (6) and (8) are kept the same as before. It is observed that the breakdown curve is generally higher when d is larger even at the same pd value, which confirms the violation of the similarity law in the FE regime. Similar phenomena were also reported by Ramilović-Radjenović *et al* in [19]. The Paschen's curves are compared with and without considering the non-uniformity of the electric field. It seems that ignoring the non-uniformity of the electric field and the modification of the Townsend coefficient will shift the Paschen's minimum to a lower breakdown voltage and a lower pd value. This is due to the fact that for a fixed applied voltage, assuming a constant electric field across the gap will overestimate the electron

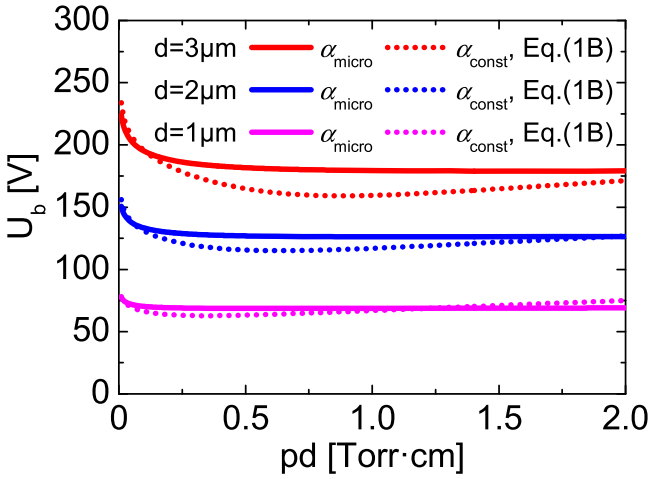

Figure 5. Calculated Paschen's curves for fixed gap distances using different Townsend coefficients. In the calculation, $\gamma_{SEE} = 0.01$ and $\beta = 50$.

avalanche contribution, which results in lower breakdown voltages. Note that since the *pd* range in figure 5 is relatively larger than that in figure 2 (for example, $pd = 0.076$ Torr cm with $d = 1$ μm and $p = 760$ Torr), the α process becomes more collisional and the electron avalanche ionization contributes more. In this situation, the difference of the Townsend coefficient matters more significantly and the difference of Paschen's curve can be clearly observed in figure 5 for larger *pd* values (or d/λ is much larger than 1).

The breakdown mode transitions with a variation of gas pressure and gap distance are shown in figure 6. The numerical values are obtained by solving equation (11), varying the gas pressure from 10 to 5000 Torr and the gap distance from 1 to 50 μm. In figure 6(a), it is shown that the discharge is dominated by field emission when the gap distance is less than ~10 μm. The dashed contour lines clearly show the breakdown mode transitions with different p and d. In figure 6(b), it can be seen that field emission remains in a larger gap at lower pressures, which delays the breakdown mode transition. At high pressures (>1000 Torr), increasing the gas pressure does not change breakdown mode transition points, which stay roughly at the same gap distance. For the atmospheric pressure microgaps, when the gap distance is larger than 10 μm, field emission is ignorable. The results illustrate the dependence of the breakdown characteristics and the mode transitions with the evolution of field emission on gas pressure and gap distance, which is a more complete way compared to previous studies.

The effect of the cathode field enhancement on the Paschen's curve is shown in figure 7. In the calculations in figure 7(a), the gap distance is fixed at 1 and 3 μm and the field enhancement factor β is chosen as 10, 50, and 100. The Paschen's curve is found to be quite sensitive to the field enhancement factor β. Taking the case of $d = 1$ μm for example, the breakdown voltage with $\beta = 10$ can be an order of magnitude larger than that with $\beta = 100$. This is because the large field enhancement increases the field emission current, which lowers the breakdown voltage. With the same gap distance, the larger field enhancement will flatten the shape of

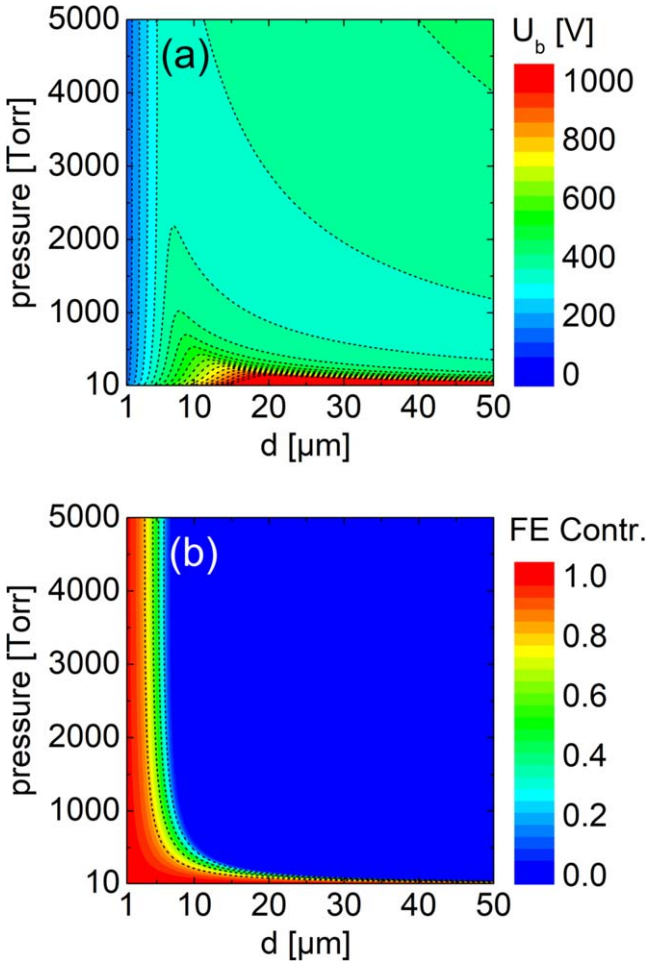

Figure 6. (a) The breakdown voltage versus the pressure p and gap distance d; (b) the transition from the field emission to the secondary electron emission. In the calculation, $\gamma_{SEE} = 0.01$ and $\beta = 50$.

the breakdown curves, i.e., the breakdown voltage weakly depends on gas pressure. Note that for the 3 μm gap with $\beta = 10$, the breakdown curve is exactly the same as the Paschen's curve from equation (11) assuming the field emission coefficient equals to zero. This tells us that, if the field enhancement is not sufficiently high, field emission will not contribute to gas breakdown even in a gap of several microns. Or equivalently, with a smaller field enhancement factor, the field emission can disappear earlier as the gap distance increases. To confirm this, the Paschen's curves for constant pressure with $\beta = 10$, 50, and 100 are calculated and shown in figure 7(b). It can be seen that the critical distance of the breakdown mode transition becomes smaller as β decreases. Besides that, in the SEE regime, the conventional Paschen's curves with different β are no longer the same. This is because the Townsend ionization coefficient is spatially determined by the electric field distribution, which captures the difference in electron avalanche contribution when the electric field non-uniformity is considered. It is observed that in the FE regime, a larger β will lower the breakdown voltage, whereas in the SEE regime, a larger β will increase the breakdown voltage, which was not included in the previous model. Note that although the avalanche process in the

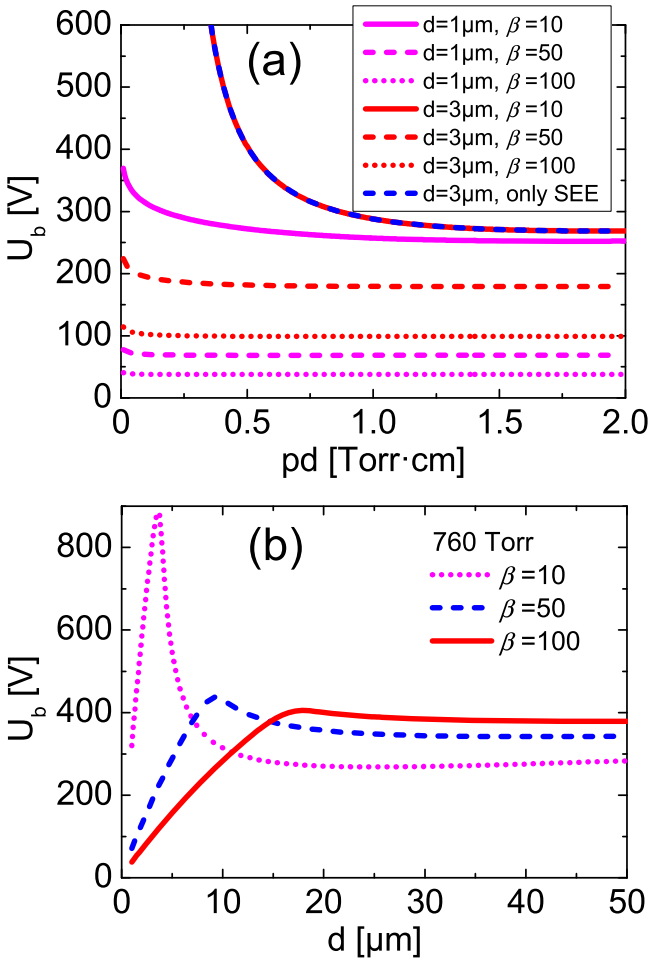

Figure 7. The effect of the field enhancement factor on the Paschen's curves. (a) Gap distance is fixed at 1 and 3 μm with different field enhancement factors; (b) gas pressure is fixed at 760 Torr with different field enhancement factors.

cathode region is stronger with a larger β, the integral of the electron avalanche across the gap could still be smaller since the electric field is suppressed elsewhere for a given applied voltage, which explains the higher breakdown voltages with a larger β in the SEE regime. It is interesting to note that the in the FE-driven regime, Townsend coefficient could also be considered as a modifier on field emission (or field enhancement), which could amplify the field emission current density j_{FE} from the cathode wall. The growth in current density j will be approximated by

$$j \approx \frac{j_{\mathrm{FE}} \exp\left(\int_0^d \alpha(x)\cdot \mathrm{d}x\right)}{1-\gamma_{\mathrm{eff}}\left[\exp\left(\int_0^d \alpha(x)\cdot \mathrm{d}x\right)-1\right]}, \qquad (14)$$

where $\gamma_{\mathrm{eff}} = \gamma_{\mathrm{SEE}} + \gamma_{\mathrm{FE}}$ is the effective SEE coefficient [12, 39]. This is based on that a single ion may both contribute to the ion-impact SEE and ion-enhanced field emission, even though they are independent mechanisms [21, 22]. Then, regardless of the source of current and in case of $\lambda \sim 1/\alpha$, one could also obtain a relation for the transition point versus the total emission current, as well as the mean free path, when, between two consecutive collisions, electron restored energy is larger than the ionization potential and no elastic collisions occur [39–43].

Another related improvement regarding the treatment of the electric field distribution has been made with the consideration of the space charge effect in [38]. Using Taylor's series expansion, the small component of the electric field enhanced by the space charge was included and the breakdown criterion is improved in a more closed form. However, under certain conditions, some discrepancies may not be avoided since a constant charge density distribution across half of the gap is assumed to calculate the electric field at the cathode. With the incorporated electric field distribution, the present model can reveal the breakdown mode transition characteristics related to the field non-uniformity straightforwardly. When the space charge effect is less important, the improved method can apply to any geometry gap, for example, the spatially dependent fields in coaxial systems, since the electric field distribution in equation (8) could be nominal which can be obtained numerically before calculating the breakdown voltages.

4. Conclusions

The breakdown mode transitions between the FE regime and the SEE regime in microgaps are evaluated using a mathematical model considering the effect of the electric field non-uniformity. The first Townsend ionization coefficients are quantified using different empirical expressions and the Paschen's curves are obtained for variations of gas pressure and gap distance. In atmospheric microgaps, the modification of the first Townsend ionization coefficient shows impact only in small gaps or when the d/λ is not much larger than 1. Ignoring the non-uniformity of the electric field will overestimate the electron avalanche contribution and therefore underestimate the breakdown voltage. When Paschen's curves are obtained with gap distance fixed and gas pressure varied, it is found that ignoring the non-uniformity of the electric field and the modification of the Townsend coefficient will shift the Paschen's minimum point to a lower breakdown voltage at a lower pd value. The critical gap distance for the breakdown mode transition tends to increase at lower pressures, whereas it is roughly constant at higher pressures. Also, the critical point of the breakdown mode transition is shifted by the field enhancement factor computed with the non-uniform electric field. A larger β will lower the breakdown voltage in the FE regime, and increase the breakdown voltage in the SEE regime. Instead of assuming a constant electric field across the gap, the present model considering the electric field non-uniformity provides more details of the modified Paschen's curve, including the critical point of the breakdown mode transition and the breakdown behavior with various electric field distributions.

Acknowledgments

This work was supported by the Air Force Office of Scientific Research (AFOSR) MURI Grant FA9550-18-1-0062, the

DOE Plasma Science Center Grant DE-SC0001939, and an MSU Strategic Partnership Grant. Peng Zhang was also supported by AFOSR YIP Award No. FA9550-18-1-0061.

ORCID iDs

Yangyang Fu https://orcid.org/0000-0001-9593-3177
Janez Krek https://orcid.org/0000-0002-0295-0232
Peng Zhang https://orcid.org/0000-0003-0606-6855

References

[1] Peschot A, Bonifaci N, Lesaint O, Valadares C and Poulain C 2014 *Appl. Phys. Lett.* **105** 123109
[2] Radmilovic-Radjenovic M and Radjenovic B 2007 *IEEE Trans. Plasma Sci.* **35** 1223
[3] Loveless A M and Garner A L 2017 *Phys. Plasmas* **24** 113522
[4] Semnani A, Venkattraman A, Alexeenko A A and Peroulis D 2013 *Appl. Phys. Lett.* **102** 174102
[5] Li Y, Tirumala R, Rumbach P and Go D B 2013 *IEEE Trans. Plasma Sci.* **41** 24
[6] Boeuf J P, Pitchford L C and Schoenbach K H 2005 *Appl. Phys. Lett.* **86** 071501
[7] Schoenbach K H and Becker K 2016 *Eur. Phys. J. D* **70** 29
[8] Fu Y, Zhang P and Verboncoeur J P 2018 *Appl. Phys. Lett.* **112** 254102
[9] Loveless A M and Garner A L 2016 *Appl. Phys. Lett.* **108** 234103
[10] Tan X and Go D B 2018 *J. Appl. Phys.* **123** 063303
[11] Marić D, Kutasi K, Malović G and Petrović Z L 2003 *J. Phys. D: Appl. Phys.* **36** 2639
[12] Radmilović-Radjenović M, Matejčik Š, Klas M and Radjenović B 2013 *J. Phys. D: Appl. Phys.* **46** 015302
[13] Fu Y, Zhang P and Verboncoeur J P 2018 *Appl. Phys. Lett.* **113** 054102
[14] Kisliuk P 1954 *J. Appl. Phys.* **25** 897
[15] Boyle W S and Kisliuk P 1955 *Phys. Rev.* **97** 255
[16] Kisliuk P 1959 *J. Appl. Phys.* **30** 51
[17] Germer L H 1959 *J. Appl. Phys.* **30** 46
[18] Radmilović-Radjenović M and Radjenović B 2007 *Plasma Sources Sci. Technol.* **16** 337
[19] Radmilović-Radjenović M and Radjenović B 2008 *Plasma Sources Sci. Technol.* **17** 024005
[20] Radmilović-Radjenović M and Radjenović B 2008 *Europhys. Lett.* **83** 25001
[21] Go D B and Pohlman D A 2010 *J. Appl. Phys.* **107** 103303
[22] Tirumala R and Go D B 2010 *Appl. Phys. Lett.* **97** 151502
[23] Fowler R and Nordheim L 1928 *Proc. R. Soc.* A **119** 173
[24] Go D B and Venkattraman A 2014 *J. Phys. D: Appl. Phys.* **47** 503001
[25] Fu Y, Yang S, Zou X, Luo H and Wang X 2016 *Phys. Plasmas* **23** 093509
[26] Fu Y, Yang S, Zou X, Luo H and Wang X 2016 *High Voltage* **1** 86
[27] Fu Y, Yang S, Zou X, Luo H and Wang X 2017 *Phys. Plasmas* **24** 023508
[28] Lisovskiy V A, Osmayev R O, Gapon A V, Dudin S V, Lesnik I S and Yegorenkov V D 2017 *Vacuum* **145** 19
[29] Noori H and Ranjbar A H 2017 *Phys. Plasmas* **24** 103527
[30] Townsend J S 1915 *Electricity in Gases* (Oxford: Oxford University Press)
[31] Paschen F 1889 *Ann. Phys.* **273** 69
[32] Raizer Y P 1991 *Gas Discharge Physics* (New York: Springer)
[33] Spindt C, Brodie I, Humphrey L and Westerberg E 1976 *J. Appl. Phys.* **47** 5248
[34] Rodriguez A, Morgan W, Touryan K and Moeny W 1991 *J. Appl. Phys.* **70** 2015
[35] Tsang W M and Wong S P 2002 *Appl. Phys. Lett.* **81** 3942
[36] Mackie W A, Hartman R L, Anderson M A and Davis P R 1994 *J. Vac. Sci. Technol.* B **12** 722
[37] Slade P G and Taylor E D 2002 *IEEE Trans. Compon. Packag. Technol.* **25** 390
[38] Venkattraman A and Alexeenko A A 2012 *Phys. Plasmas* **19** 123515
[39] Rumbach P, Li Y, Martinez S, Twahirwa T J and Go D B 2014 *Plasma Sources Sci. Technol.* **23** 065026
[40] Feng Y and Verboncoeur J P 2005 *Phys. Plasmas* **12** 103301
[41] Feng Y and Verboncoeur J P 2006 *Phys. Plasmas* **13** 073105
[42] Davydov Y I 2006 *IEEE Trans. Nucl. Sci.* **53** 2931
[43] Feng Y, Verboncoeur J P and Lin M C 2008 *Phys. Plasmas* **15** 043301